Supplementary data

Supplementary Figure S1. Most ribosome-associated miRNAs show medium occupancy and may share common biological functions. A-B) Polysomal profile of REN cells in the absence (A) and in the presence (B) of EDTA. Ribosomal subunits are evidenced. Fractions pooling is indicated. C) Heatmap of miRNAs polysome occupancy on EDTA treated and untreated REN cells: the bulk of miRNAs exhibit a medium occupancy. D) Correlation analysis between miRNAs occupancy and miRNAs expression levels reveals that the two factors are not associated (R^2= 0.35182). E) *In silico* pathways analysis has been performed using MirSystem (http://mirsystem.cgm.ntu.edu.tw/) on line tool on the most significant polysomes associated miRNAs.

Supplementary Figure S2. miR-24-3p is expressed in lung and breast cancer cells. Real time PCR evidences that miR-24-3p is expressed also in the indicated lung and breast cancer cell lines, at different levels. MPM indicates a pool of Mesothelioma cell lines. Values represent the mean ± SD.

Supplementary Figure S3. miR-24-3p knockdown mildly affects cell proliferation and does not influence the apoptotic rate of MPM cell lines. A) qRT-PCR indicates that transduction of miR-Zip-24 reduces miR-24-3p expression in REN, MM98 and MSTO-211H cells. miR-empty is used as control. B) CTB viability assay on REN, MM98 and MSTO-211H indicates that a partial depletion of miR-24-3p reduces MPM cell lines proliferation, at the indicated time points. C) FACS analysis shows that the apoptotic rate is similar in all conditions evaluated in REN, MM98 and MSTO-211H cells. MPM cells treated with Staurosporin are used as positive control for apoptosis. D) Cell cycle analysis of REN, MM98 and MSTO-211H cells with normal or depleted miR-24-3p expression. All values represent the mean ± SD of three independent experiments. p-values, obtained by two-tailed Student's t-test, are indicated (*$p \leq 0.05$; **$p \leq 0.01$).

Supplementary Figure S4. miR-24-3p fosters cells migration capability. A) Representative images of wound-healing assay on MSTO-211H cells show that miR-24-3p knockdown reduces cells migration, compared to miR-empty, used as control. B) qRT-

PCR evidences transduction efficiency of miR-24-3p in MeT-5A cells. C-D) Representative images of wound-healing assay on breast MCF7 cells after partial depletion (C) and overexpression (D) of miR-24-3p confirm that miR-24-3p has a promigratory role. Results are representative of three independent experiments. p-value, obtained by Student t-test, is indicated (***$p \leq 0.001$). Scale bar corresponds to 10μm.

Supplementary Figure S5. RNA-seq analysis on miR-24-3p knockdown REN and MM98 cells. A) Upregulated genes are categorized in protein coding genes, pseudogenes, lncRNAs and antisense RNAs, showing similar percentage in both REN and MM98 cell lines. B) Schematic of miR-24-3p putative direct targets derived from bioinformatic/NGS crossing analysis (details in the text). C) PRECOG analysis on selected miR-24-3p regulated genes, assessed by mean meta-*z*-scores, shows that they are associated with favorable survival in most considered cancer types. D) Real Time PCR analysis of indicated migration involved mRNA targets confirms upregulation when miR-24-3p is inhibited, both in REN, MM98 and MSTO-211H cells. E) qRT-PCR on MeT-5A cells illustrates that indicated targets are downregulated in miR-24-3p overexpression condition. F) Actinomycin D treatment of MPM miR-Empty and MPM miR-Zip24 cells indicates that knockdown of miR-24-3p results in an expected increase of CGN mRNA stability.

Supplementary Figure S6. CXADR and BCAM mRNA distribution in REN polysomes. A) CXADR mRNA distribution in REN miR-empty and miR-Zip-24 cells shows that CXADR mRNA is more translated in miR-24-3p knockdown conditions. B) Similar results were obtained for BCAM mRNA. Values represent the mean ± SD. All experiments are performed as biological replicates. p-values, obtained by two-tailed Student's t-test, are indicated (*$p \leq 0.05$; **$p \leq 0.01$; ***$p \leq 0.001$).

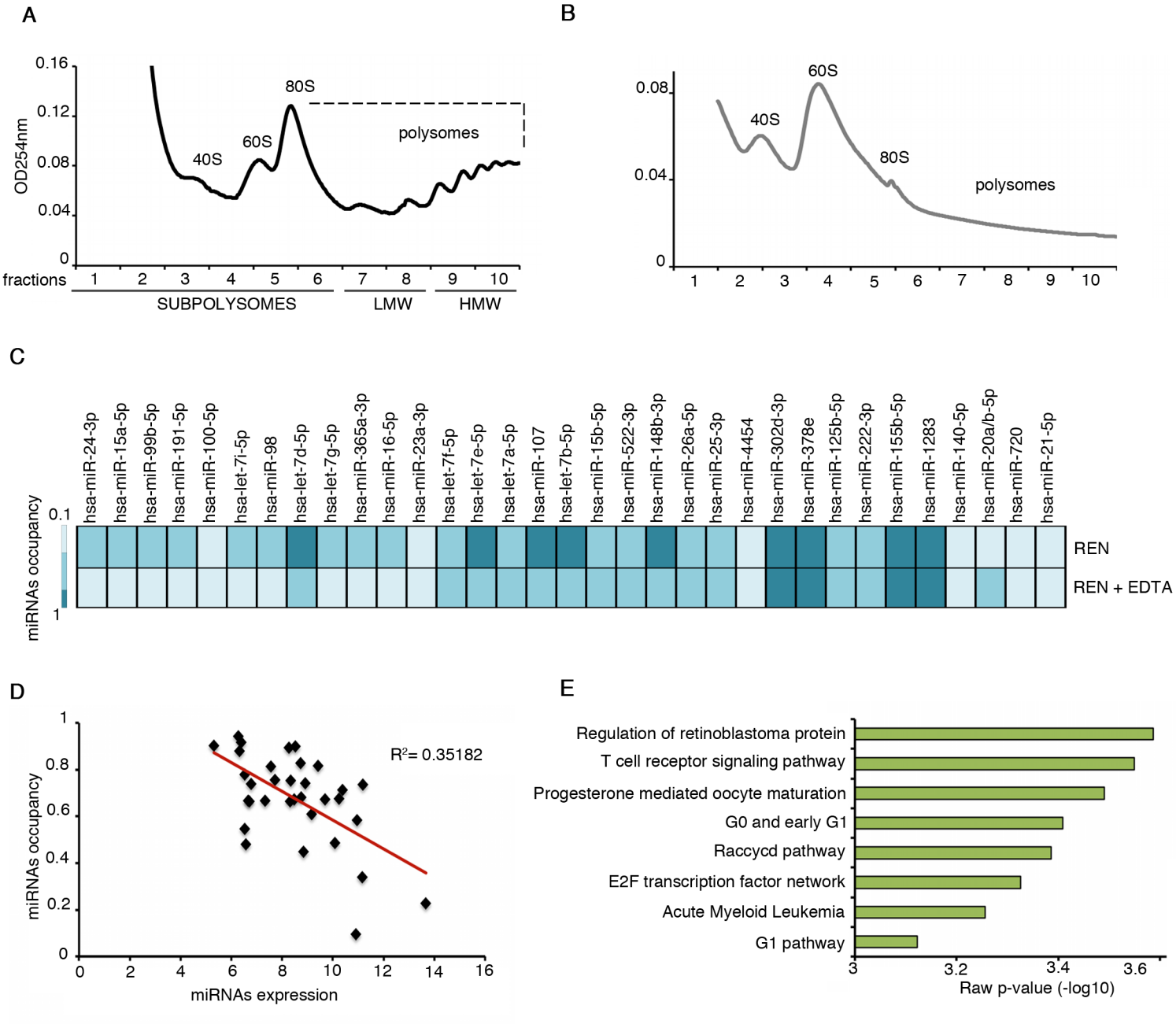
A
0.16
0.12
0.08
0.04
0
OD254nm
40S
60S
80S
polysomes
fractions 1 2 3 4 5 6 7 8 9 10
SUBPOLYSOMES
LMW
HMW
B
0.08
0.04
0
60S
40S
80S
polysomes
1 2 3 4 5 6 7 8 9 10
C
hsa-miR-24-3p
hsa-miR-15a-5p
hsa-miR-99b-5p
hsa-miR-191-5p
hsa-miR-100-5p
hsa-let-7i-5p
hsa-miR-98
hsa-let-7d-5p
hsa-let-7g-5p
hsa-miR-365a-3p
hsa-miR-16-5p
hsa-miR-23a-3p
hsa-let-7f-5p
hsa-let-7e-5p
hsa-let-7a-5p
hsa-miR-107
hsa-let-7b-5p
hsa-miR-15b-5p
hsa-miR-522-3p
hsa-miR-148b-3p
hsa-miR-26a-5p
hsa-miR-25-3p
hsa-miR-4454
hsa-miR-302d-3p
hsa-miR-378e
hsa-miR-125b-5p
hsa-miR-222-3p
hsa-miR-155b-5p
hsa-miR-1283
hsa-miR-140-5p
hsa-miR-20a/b-5p
hsa-miR-720
hsa-miR-21-5p
miRNAs occupancy
0.1
1
REN
REN + EDTA
D
1
0.8
0.6
0.4
0.2
0
miRNAs occupancy
R²= 0.35182
0 2 4 6 8 10 12 14 16
miRNAs expression
E
Regulation of retinoblastoma protein
T cell receptor signaling pathway
Progesterone mediated oocyte maturation
G0 and early G1
Raccycd pathway
E2F transcription factor network
Acute Myeloid Leukemia
G1 pathway
3 3.2 3.4 3.6
Raw p-value (-log10)

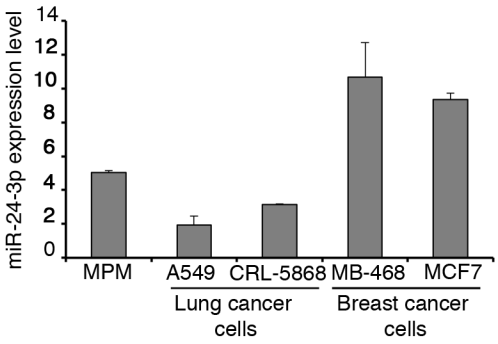
miR-24-3p expression level
14
12
10
8
6
4
2
0
MPM
A549
CRL-5868
MB-468
MCF7
Lung cancer cells
Breast cancer cells

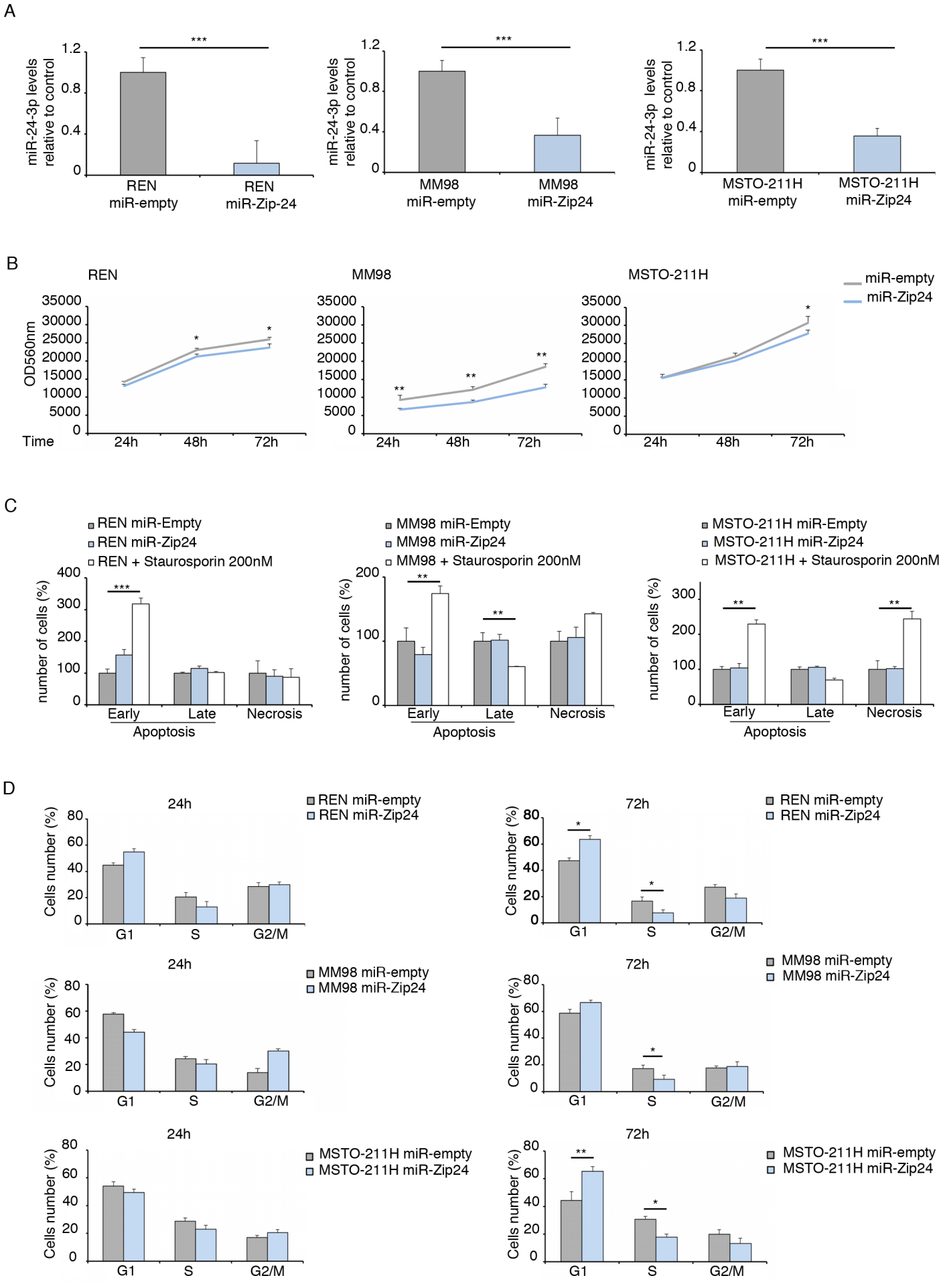
A
miR-24-3p levels relative to control
1.2
0.8
0.4
0
***
REN miR-empty
REN miR-Zip-24
MM98 miR-empty
MM98 miR-Zip24
MSTO-211H miR-empty
MSTO-211H miR-Zip24
B
REN
MM98
MSTO-211H
miR-empty
miR-Zip24
OD560nm
35000
30000
25000
20000
15000
10000
5000
0
Time
24h
48h
72h
C
REN miR-Empty
REN miR-Zip24
REN + Staurosporin 200nM
MM98 miR-Empty
MM98 miR-Zip24
MM98 + Staurosporin 200nM
MSTO-211H miR-Empty
MSTO-211H miR-Zip24
MSTO-211H + Staurosporin 200nM
number of cells (%)
Early
Late
Necrosis
Apoptosis
D
24h
72h
REN miR-empty
REN miR-Zip24
MM98 miR-empty
MM98 miR-Zip24
MSTO-211H miR-empty
MSTO-211H miR-Zip24
Cells number (%)
G1
S
G2/M

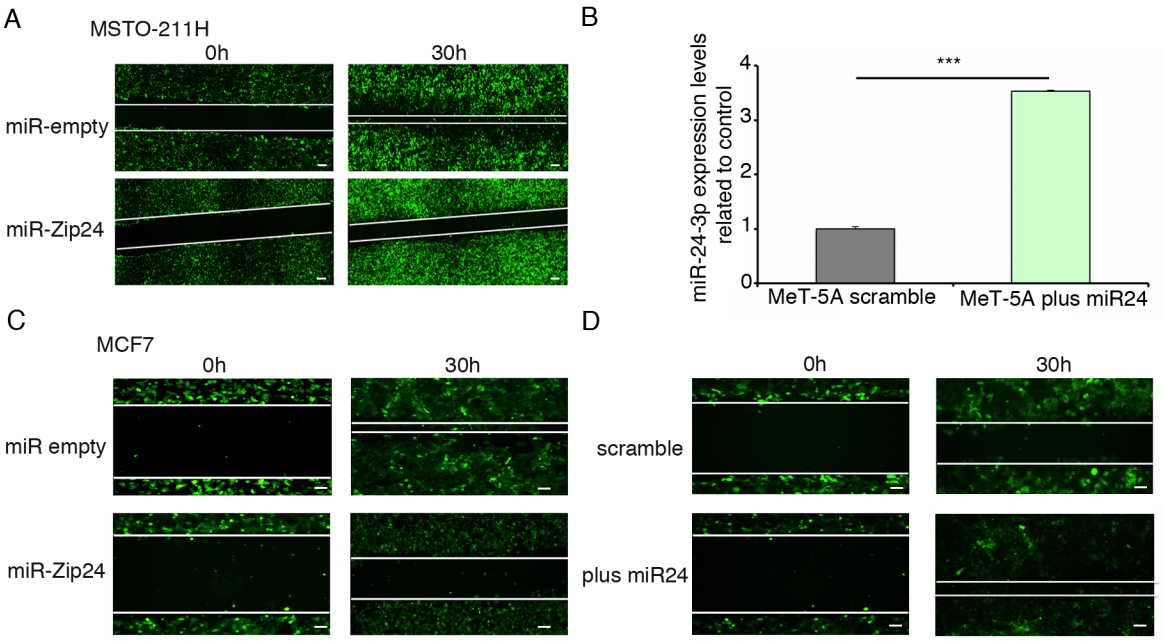
A
MSTO-211H
0h
30h
miR-empty
miR-Zip24
B
miR-24-3p expression levels related to control
***
MeT-5A scramble
MeT-5A plus miR24
C
MCF7
0h
30h
miR empty
miR-Zip24
D
0h
30h
scramble
plus miR24

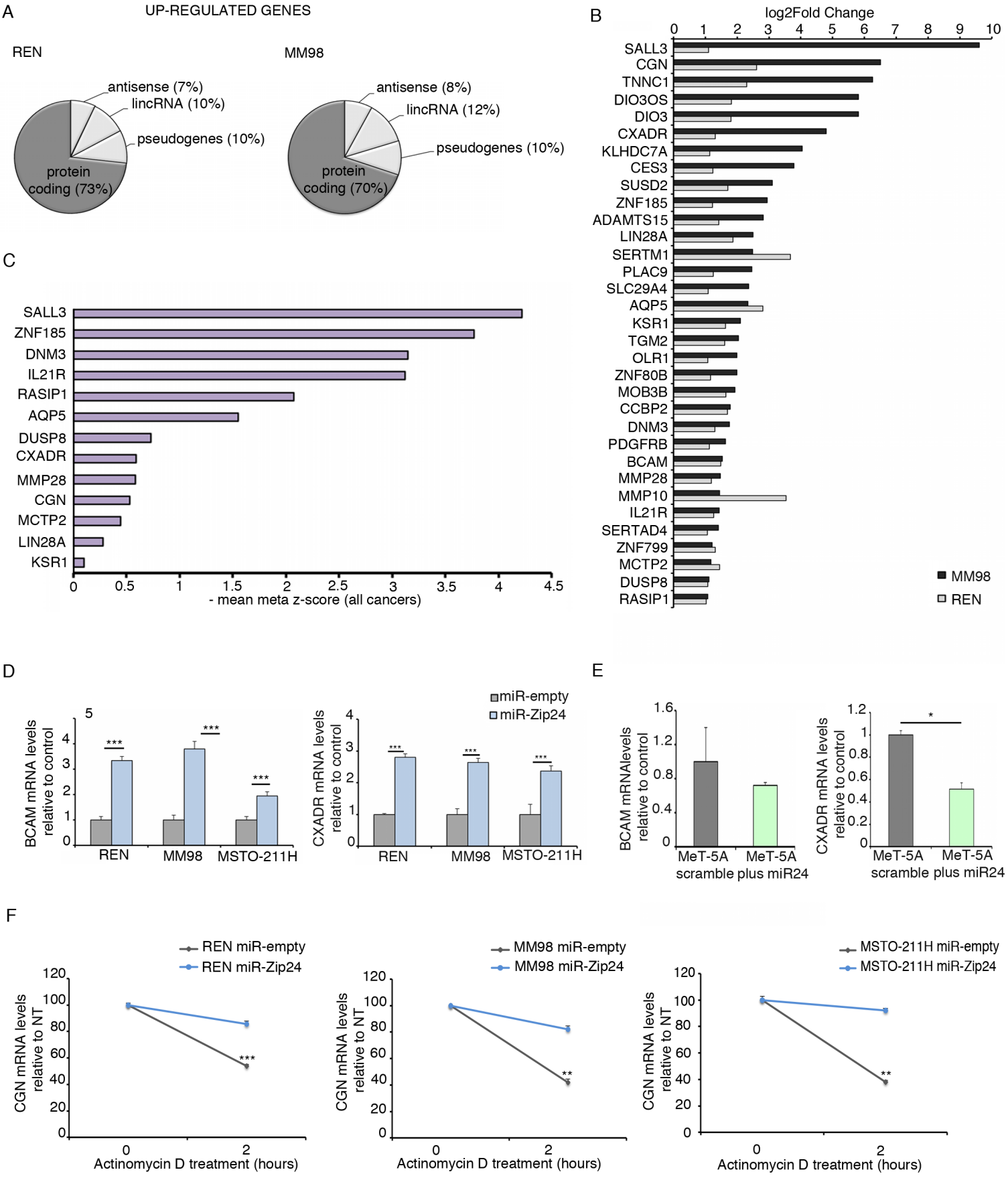
A
UP-REGULATED GENES
REN
antisense (7%)
lincRNA (10%)
pseudogenes (10%)
protein coding (73%)
MM98
antisense (8%)
lincRNA (12%)
pseudogenes (10%)
protein coding (70%)
B
log2Fold Change
0 1 2 3 4 5 6 7 8 9 10
SALL3
CGN
TNNC1
DIO3OS
DIO3
CXADR
KLHDC7A
CES3
SUSD2
ZNF185
ADAMTS15
LIN28A
SERTM1
PLAC9
SLC29A4
AQP5
KSR1
TGM2
OLR1
ZNF80B
MOB3B
CCBP2
DNM3
PDGFRB
BCAM
MMP28
MMP10
IL21R
SERTAD4
ZNF799
MCTP2
DUSP8
RASIP1
MM98
REN
C
SALL3
ZNF185
DNM3
IL21R
RASIP1
AQP5
DUSP8
CXADR
MMP28
CGN
MCTP2
LIN28A
KSR1
0 0.5 1 1.5 2 2.5 3 3.5 4 4.5
- mean meta z-score (all cancers)
D
BCAM mRNA levels relative to control
REN
MM98
MSTO-211H
miR-empty
miR-Zip24
CXADR mRNA levels relative to control
REN
MM98
MSTO-211H
E
BCAM mRNAlevels relative to control
MeT-5A
MeT-5A
scramble plus miR24
CXADR mRNA levels relative to control
MeT-5A
MeT-5A
scramble plus miR24
F
REN miR-empty
REN miR-Zip24
CGN mRNA levels relative to NT
Actinomycin D treatment (hours)
MM98 miR-empty
MM98 miR-Zip24
CGN mRNA levels relative to NT
Actinomycin D treatment (hours)
MSTO-211H miR-empty
MSTO-211H miR-Zip24
CGN mRNA levels relative to NT
Actinomycin D treatment (hours)

A

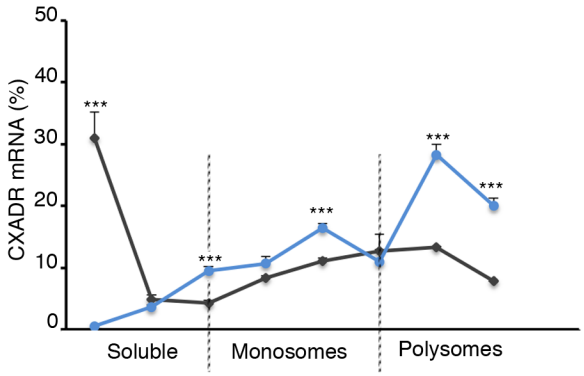
CXADR mRNA (%)
50
40
30
20
10
0
***
***
***
***
***
Soluble
Monosomes
Polysomes

B

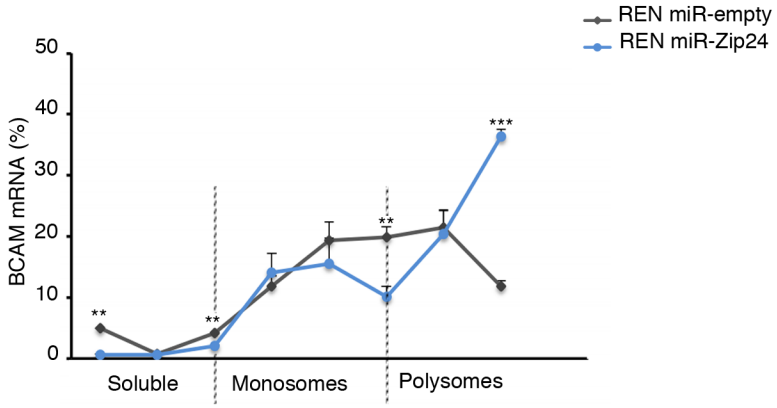
REN miR-empty
REN miR-Zip24
BCAM mRNA (%)
50
40
30
20
10
0
**
**
**
***
Soluble
Monosomes
Polysomes

Supplementary Table S1. Autopsies of NOD-SCID mice 30 days after I.P. REN injection. The number of autopsies is indicated for each group. Weights value represent the mean ± SD.

Group	Weight (grams)			Metastasis	Ascite	Hemorrage
	Body	Diaphragm	Tumor mass			
miR-empty mice (n=6)	30,45 ± 1,68	0,30 ± 0,13	0,54 ± 0,16	High abundance, enlarged limphonodes	Massive	Massive
miR-Zip24 mice (n=6)	27,75± 2,42	0,16 ± 0,09	0,20 ± 0,12	Low abundance	Mild	ND